ASSESSING THE HEALTH OF *PINUS RADIATA* PLANTATIONS USING REMOTE SENSING DATA AND DECISION TREE ANALYSIS

NEIL C. SIMS*,

Ensis,
Private Bag 10, Clayton South, Victoria, Australia, 3169

CHRISTINE STONE,

New South Wales Department of Primary Industries Science and Research,
P. O. Box 100, Beecroft, NSW, Australia, 2119

NICHOLAS C. COOPS,

Department of Forest Resource Management,
University of British Columbia, Vancouver, Canada, 2424 Main Mall, V6T 1Z4

and PHILIP RYAN

formerly of CSIRO Division of Forestry and Forest Products
Private Bag 10, Clayton South, Victoria, Australia, 3169

(Received for publication 13 February 2006; revision 19 July 2006)

ABSTRACT

Forest health monitoring is essential to sustainable management of *Pinus radiata* D. Don plantations. Conventional survey techniques such as aerial sketch mapping are qualitative and subjective, their effectiveness depending on the skill of the surveyor. In contrast, digital remote sensing has the potential to provide quantitative and objective data on the location, extent, and severity of crown damage at a range of spatial scales. Decision tree analysis can incorporate both categorical and continuous data and is inherently non-parametric. Decision trees were used to model the crown condition of *P. radiata* plantations in southern New South Wales in three situations involving discoloured leaves, stunted crowns, and transparent crowns associated respectively with the *Diplodia pinea* (Desm.) Kickx fungus, nitrogen deficiency, and the pine aphid *Essigella californica* Essig. Spectral indices and fraction images derived from linear spectral mixture analyses of remote sensing scenes were used to classify crowns into either two or three condition classes. The best performing model was obtained for *D. pinea* with a two-class classification of crown discoloration (overall accuracy [OA] 92%; Kappa 83%). The three-class model of crown transparency from

* Corresponding author: Neil.Sims@ensisjv.com

E. californica defoliation was moderately accurate (OA 68%, Kappa 28%), while the weakest model was a two-class model of crown volumes affected by soil nitrogen levels (OA = 58%, Kappa = 21%). Correlation between modelled outputs and environmental spatial variables revealed a high correlation between net solar radiation levels and crown transparency classes due to *E. californica* defoliation.

Keywords: remote sensing; decision tree; forest health; New South Wales; *Pinus radiata; Diplodia pinea; Essigella californica*.

INTRODUCTION

The productivity of Australian softwood plantations is limited by a range of abiotic and biotic factors that affect the health of the forests (Nambiar & Booth 1991; Neumann & Marks 1990; May & Carlyle 2003). Management of these damaging factors requires quantification of their distribution and severity throughout plantations. However, the accuracy and effectiveness of current methods of forest health assessment, such as aerial sketch-mapping of affected stands on hardcopy maps, is often highly dependent on surveyor skill (McConnell *et al.* 2000; White *et al.* 2005*)* and the information is difficult to integrate into plantation management procedures. Developing quantitative relationships between stand growth and a spatially explicit determination of canopy health using remotely sensed data will enable plantation managers to account accurately for the impact of damaging agents and processes in their inventory management and spatial harvest scheduling systems. This paper presents a preliminary analysis of high-resolution remotely sensed data for the detection and classification of a range of crown damage symptoms observed in *P. radiata* plantations.

Digital remote sensing systems measure the amount of electromagnetic energy reflected and/or emitted from a target within one or more wavelength bands (Asrar 1989). Improvements in remote sensing technologies, particularly in the spatial and spectral resolution of optical sensors, have made the prospect of using digital remotely sensed imagery to detect and classify vegetation health a realistic and attractive option (Franklin 2000). Recent studies have successfully related a range of vegetative biochemical (e.g., chlorophyll content) and biophysical attributes (such as green biomass and leaf area index) to spectral algorithms extracted from remotely sensed imagery (Martin & Aber 1997; White *et al*. 1997; Pu *et al.* 2005). However, less work has been directed specifically at relating remotely sensed data to crown chlorosis, discoloration, or defoliation (Hall *et al*. 2003; Leckie *et al.* 2005; Pontius *et al.* 2005; White *et al*. 2005). A number of different approaches have been used to detect and classify vegetation health from remote sensing imagery, including spectral indices and spectral un-mixing. Spectral indices are often computed by comparing variations in red reflectance, due to reduced chlorophyll absorption, to decreases in near infrared (NIR) reflectance from

reduced cellular integrity. These indices are related to the functioning of internal plant processes such as pigment content (Thenkabail *et al.* 2000; Zarco-Tejada *et al.* 2003, 2004; Coops *et al.* 2004) and crown biomass (Schlerf *et al.* 2005). The derivation of spectral algorithms has developed rapidly, especially when using hyperspectral or continuous spectral data derived through the application of radiative transfer models (Zarco-Tejada *et al.* 2004). Many of these algorithms incorporate features associated with the spectral red edge (Fig. 1). Red-edge indices examine reflectance at wavelengths between 690 and 740 nm (Curran *et al.* 1990) where reflectance is highly sensitive to strong absorption by chlorophyll in the red region and strong reflectance in the NIR region, due to scattering in the leaf mesophyll and the absence of absorption by pigments (Gausman 1985; Curran *et al.* 1990). Increased absorption by chlorophyll creates a deeper and broader absorption feature around 680 nm (Fig. 1) extending into longer wavelengths, which changes the slope of the lower part of the red edge curve. The magnitude of NIR reflectance is sensitive to leaf moisture content and canopy structure (Knipling 1970), with increased canopy moisture levels tending to reduce NIR reflectance, and increased structural complexity of the canopy tending to increase NIR reflectance. These characteristics tend to affect the slope of the upper part of the red-edge curve. Thus, the shape of the red edge can indicate the condition of foliage.

In addition to spectral information, embedded in the imagery is information related to its textural composition. An alternative approach to the application spectral

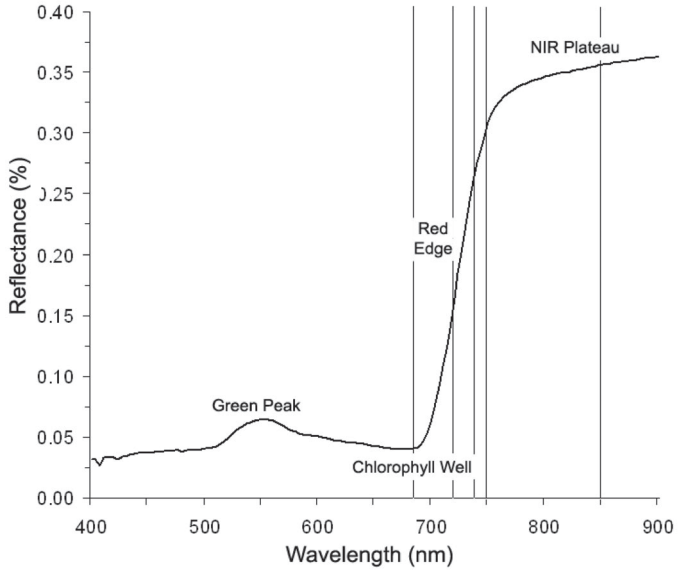

FIG. 1–Typical mean spectrum of a healthy *Pinus radiata* needle in visible and NIR wavelengths showing the spectral location of bands used in this analysis.

indices is an image transformation technique termed linear spectral unmixing. Spectral unmixing is based on the assumption that the spectrum of a mixed pixel has been created by the linear superposition of the spectra of the pure components, and the coefficients of the linear superposition are equal to the fractional coverages of the field of view of the pixel by the corresponding pure components (Tompkins *et al.* 1997). Endmembers calculated in forestry applications often include canopy vegetation, bare soil, and shadow (Lévesque & King 2003). Studies have shown that these endmembers are highly correlated with canopy structure (Peddle *et al.* 1999) and account for a large proportion of the spectral variation between pixels in remotely sensed images for forestry (Roberts *et al*. 1993; Fitzgerald *et al.* 2002; Lévesque & King 2003). A benefit of the approach is that non-vegetated components can be explicitly accounted for at the sub-pixel scale (Peddle *et al.* 1999), which can be important, especially with low stem density or thin open canopies where the background surface dominates the signal (Goodwin *et al.* 2005).

Concurrent with these developments in extracting relevant information from remotely acquired imagery, is the increasing use of different modelling methodologies. Decision trees, also known as Classification and Regression Trees (CART), are exploratory tools that can be used to identify numerical classifications using a number of input variables. Decision trees offer a number of advantages over modelling methods based on standard regression and statistical inference, including the capability to encapsulate a range of variables (e.g., categorical, ordinal, and continuous) in an easy to understand, coherent structure, and have been applied to numerous data sets derived from remote sensing (Hansen *et al.* 1996; Friedl & Brodley 1997; Lawrence & Wright 2001; Rosso & Hansen 2004). However, while decision tree methods are nonparametric and nonlinear, their empirical nature does not allow formal procedures of inference amongst the independent variables; therefore, they are poor at extrapolating beyond the learning sample (Lees 1994).

This article describes a pilot study established to assess the capacity of high spatial resolution, narrow-band, multi-spectral, airborne imagery to detect and classify a range of common symptoms associated with crown health of *P. radiata* plantations in southern New South Wales. It describes methods for quantifying crown damage of *P. radiata* affected by three stresses — namely, the fungal pathogen *Diplodia pinea*, low soil nitrogen levels, and the Californian pine aphid *Essigella californica*. It then presents an approach to extracting predictor variables from the imagery; the predictor variables were used to create decision tree models predicting broad categories of crown condition based on the crown damage assessments. Finally, the modelled spatial coverages were correlated to a range of terrain, climatic, geological, and soil geographic information system (GIS) attributes, and their correlation coefficients were compared.

MATERIALS AND METHODS

Study Area

The Carabost (–35°39´S, 147°49´E; 500 m elevation) and Buccleuch (–35°06´S, 148°17´E; 450 m elevation) plantations cover 13 137 and 31 666 ha respectively in southern NSW. Annual rainfall in this region is less than 700 mm and the majority of the precipitation occurs in winter, with summers hot and dry. This area is generally regarded as marginal for *P. radiata* growth and these plantations have a history of exposure to a range of damaging factors. Three sites were selected for this pilot study, based on the distribution of the different damaging factors: the Kangaroo Vale section of Buccleuch State Forest (*D. pinea*); near Strip Road (*E. californica*); and Downfall Creek (nitrogen) within Carabost State Forest.

Field Sampling Strategy

Field data collection occurred 1 week after initial image capture (explained in detail below) in 2002 and concurrent with image capture in 2003. Imagery was obtained prior to the field programme in 2002 to ensure individual tree crowns were correctly co-located in the field and on the imagery, as co-locating tree crowns in the field without imagery has proved difficult (Coops *et al*. 2003). The expression of crown symptoms caused by damaging agents such as defoliation by *E. californica* is most acute at the end of winter (Neumann & Marks 1990; Nambiar & Booth 1991; May & Carlyle 2003) when mature foliage has been exposed to the damaging agents for approximately 1 year and new shoots (which can mask reduced condition) are avoided as they occur later in the growing season. The field team consisted of three forest health experts, one from the Forest Health Survey Unit (FHSU) of Forests NSW, with significant experience in detecting and assessing forest health in Australia and overseas. The damaging factors examined each have distinctive symptoms and/or a unique scale of attack (Table 1).

The sampling strategy used to locate and measure the crown symptoms (from healthy to dead) within the plantation varied depending on the phenology of the damaging factor. The aim was to obtain a representative sample of trees covering the full range of symptoms per agent, not to obtain a statistically balanced sample of trees over the entire estate. As a result, plot placement was positioned to ensure that enough trees with those damaging agents were sampled. Field data collection, plot placement, and data collection protocol varied for each damaging agent and will be described in detail below.

Diplodia pinea

Diplodia pinea is among the most common and widely distributed fungal pathogens of conifers (Stanosz 1997). Often a leader or outer branch shoot is affected first, resulting in dead tops followed by an increasing number of dying branches. The

TABLE 1–Characteristics of damaging factors examined in this study.

Stressor	Needle symptom	Crown symptoms	Tree attributes measured in the field	Tree attributes used in decision tree modelling
Diplodia pinea (fungal pathogen)	Necrosis	Colour change	Height, dbh (1.3 m)	Proportion of discoloration
	Colour change through pale green, yellow, red, and grey	Initial impact in one or a few outer branches progressing to whole tree	Leader colour class	Overall crown colour:
			Proportion crown discoloured (5% categories for each crown quartile and summed)	Proportional discoloration (0 = <40%, 1 = >40%).
Soil nitrogen (soil nutrient deficiency)	Chlorosis	Stunted growth	Height, dbh (1.3 m)	Conical crown volume
	Short and stunted needles	Poor crown structure	Crown transparency (10% categories)	Mean crown transparency (%)
	Pale-green to yellow needle colour		Conical crown volume (m^3)	
Essigella californica (aphid)	Chlorosis	Increased defoliation	Height, dbh (1.3 m)	Mean crown transparency: (3 classes: high >50%, moderate 25–50%, and low 0–25%)
			Proportion affected (5% categories)	
			Crown transparency (5% categories from each crown quartile).	Upper crown transparency
				Proportion of crown affected

lower crown can remain green and of normal density. The visual symptoms include needles becoming uniformly paler green (briefly) then changing colour from yellow, through orange and red, and ultimately being shed. The patchy nature of *D. pinea* infection makes random plot placement in the landscape not practical. As a result, circular plots were located around key infected "landmark" trees initially identified by the Forest Health Survey Unit and located on the imagery. Each plot was 17.2 m in radius, resulting in a 0.1-ha plot. A total of three plots were established to ensure a reasonable number of damaged trees were sampled. In addition to recording tree height, stem diameter (at 1.3 m), and leader colour, the degree of discoloration in each of the crown quartiles was recorded and tallied to provide an overall percentage of total crown discoloured.

Nitrogen soil deficiency

Nitrogen deficiency in *P. radiata*, resulting in transparent thin crowns and severe growth reductions, is normally associated with needle nitrogen concentrations of <1.2% (Carlyle & Nambiar 2001). The foliage of nitrogen-deficient trees is typically a uniform pale green, turning to yellow under severe conditions, with new needles and shoots short and stunted (Will 1985). Maps from previous forest health surveys were used to select a site with low nitrogen fertility. Total nitrogen analysis of the foliage confirmed that trees at the site were nitrogen deficient (Coops & Stone 2005). A transect sampling strategy was used to ensure that the maximum range of symptoms was sampled over the area. Transects commenced in healthy groups of trees and crossed into groups of trees showing symptoms of nitrogen deficiency, with every third tree sampled. In 2003 the site was visually assessed and it was concluded that the crown condition had not changed significantly since sampling in 2002, and field data were not collected in the second year.

Individual crown transparency was assessed in 10% increments using standardised United States Department of Agriculture Forest Service transparency cards (USDA Forest Service 2002). As crowns of deficient trees are generally smaller and shorter than crowns without major deficiency, crown and tree dimensions are a critical indicator of poor soil nitrogen status. Crown height and diameter were measured using a Vertex hypsometer and individual crown volumes were calculated. Tree diameter at breast height over bark at approximately 1.3 m and tree height were also measured.

Essigella californica (Californian pine aphid)

Essigella californica was first identified in Australia in 1998 (Carver & Kent 2000). Needle yellowing and defoliation of the mid-upper crown of older trees have been associated with *E. californica* in New South Wales, Victoria, and South Australia (Wharton & Kriticos 2004). Needles become chlorotic and fall prematurely,

starting from mid-whorl and progressing to shoot tips (May & Carlyle 2003). As severity increases, defoliation progresses up the terminal shoot and down into the lower crown, resulting in very thin crowns especially from mid to upper crown, dead tops, and green tufts of younger needles retained on the outer crown. Trees with symptoms of defoliation associated with *E. californica* were randomly located within an infected stand (tree age approximately 25 years) as the affected trees are generally uniformly distributed. Three circular plots (0.1 ha) were established ensuring that approximately 70 trees, covering the full range of symptoms, were sampled.

Tree crowns were divided into four horizontal quartiles allowing crown transparency to be assessed at each quartile. In addition, an overall crown transparency score (%) was calculated using standardised USDA Forest Service transparency cards. Needle colour provides an indication of the presence of *E. californica* and the degree of yellowing in each crown quartile was also assessed. The number of quartiles with yellowing was recorded, allowing an overall estimation of the proportion of crown affected to be assessed.

Remotely Sensed Imagery — Image Acquisition and Processing

Imagery was acquired from the Digital Multi-Spectral Camera (DMSC) II system developed by Specterra (SpecTerra Services 2004). The DMSC system has four individual 1024 × 1024 charge-coupled device arrays capable of acquiring data at 12 bit digitisation. This system can be mounted on a suitable single-engine light aircraft. Each of the four charge-coupled device arrays can be fitted with independent and replaceable narrow bandwidth (10-nm) interference filters to allow detection in selected wavelengths.

Two sets of digital multi-spectral imagery were captured. Imagery was flown in the first week of September in 2002 and 2003 under clear sky conditions with maximum solar zenith angles. September was chosen as it is just prior to the emergence of new shoot growth when mature foliage would have approximately 1 year's cumulative crown damage. The imagery was flown at the same time each year to ensure changes in sun angle would not adversely affect differences in image reflectance between dates. The importance of obtaining imagery just prior to new shoot growth was judged more critical than acquiring imagery in summer at times of maximum sun angle. In 2002, four infra-red wavelength filters allowed discrimination of the red-edge slopes (680, 720, and 740 nm) as well as near infra-red wavelength (850 nm) (Fig. 1). The bands selected in this study enabled the lower, upper, and total slopes of the red edge to be calculated as well as a simple chlorophyll ratio (Table 2). After analyses of the relationship between reflectance measurements and tree crown symptoms these wavelengths were modified in 2003 to 680, 700, 720, and 750 nm (Coops & Stone 2005). Both sets of imagery were

acquired at a pixel resolution of 0.5 × 0.5 m. The frames were then digitally mosaicked using a digital ortho-photograph as a base map with a root mean square error of 2 m.

Image Calibration

In many portions of the electromagnetic spectrum, the atmosphere has a significant effect on the surface reflectance due to scattering and absorption by gas and aerosols (Song *et al.* 2001). Correcting imagery for the effect of the atmosphere can be absolute, where the sensor signal is converted to a surface reflectance, or relative, where the same digital number in a series of corrected images is assumed to represent the same reflectance irrespective of the true ground spectra (Song *et al.* 2001). For many monitoring applications, relative radiometric normalisation is appropriate.

In this study two 4 × 4-m sheets, one of pale uniform reflectance material and one of dark, (also known as pseudo-invariant features or PIFs) were placed in open areas in the field of view of the digital multi-spectral camera in 2002 and 2003. These surfaces are assumed to be spectrally homogeneous and stable (Furby & Campbell 2001). At the time of the overpass, spectral reflectance measurements of the pseudo-invariant features were acquired with a UNISPEC spectrometer (PP Systems, Amesbury, Mass.) which measures radiation from 350 to 1100 nm. Ten reflectance measurements were averaged to obtain a mean reflectance spectrum. Using these spectra, an empirical line correction technique was then applied in an approach similar to that used by Coops *et al.* (2003) which converted the radiance of the digital multi-spectral imagery to the reflectance of the pseudo-invariant features. To ensure the two sets of imagery were correctly calibrated, reflectance brightness was then normalised to the single date standard. This was performed by identifying landcover features with a range of brightness characteristics in both the 2002 and 2003 images that were likely to have little variation in reflectance conditions over time (Furby & Campbell 2001). A regression model was then calculated between the images, using the reflectance values from the first date of imagery as the dependent variable and the raw pixel values of the second image as the independent variable. This procedure transforms pixel values in the second image data set to values commensurate with the calibrated initial scene (Yang & Lo 2000).

Crown Delineation

Once the imagery was calibrated, individual crowns were manually identified using large-scale hard copies of the imagery and field maps. Sampling of the entire crown is most appropriate for crown attribute modelling (Leckie *et al.* 1992) and therefore the full horizontal extent of each crown was delineated on the imagery, including

the sunlit and shaded components. The outline of each crown was then digitised on to the imagery from the field maps and the mean crown response of each spectral wavelength, spectral index, and fraction image was calculated and tabulated.

Modelling Crown Health using Decision Trees

The image processing software package ENVI 3.6 (RSI 2003) was used for all image analysis, including the spectral unmixing, which was undertaken following the procedures of Goodwin *et al.* (2005). A series of decision tree models were then developed and examined based on testing a single dependent continuous or categorical variable selected from the field assessments of crown health for each damaging factor (Table 1) and multiple independent variables derived from the crown spectra (i.e., the vegetation spectral indices shown in Table 2 and fraction images shown in Fig. 2). For the *D. pinea* models, the data were highly bimodal and so were transformed into binary data sets by converting proportional discoloration values lower than 40% to 0 and values greater than 40% to 1. The continuous crown transparency data recorded in crowns affected by *E. californica* were transformed into three damage classes: high (>50%), moderate (25–50%), and low (0–25%). These classes were based on those used by May & Carlyle (2003) and modified to accommodate the distribution of damage levels observed in this study.

The decision tree models were developed using CART (Classification and Regression Trees) statistical analysis software (Salford Systems 2003, version 5) applied in regression mode, which identifies natural groups using a least-squares splitting method. The objective of the pilot study was to identify broad classes of tree crown health based on key symptoms, and so the number of decision rules was limited to five. Rules were removed if they applied to only a small number of samples, or if the differences in crown condition between groups of rules were small. Models were developed using the 2002 and 2003 data, with final model development based

TABLE 2–Spectral vegetation indices calculated in this project.

	2002	2003
Lower slope	$\frac{\rho720-\rho680}{40}$	$\frac{\rho720-\rho680}{40}$
Upper slope	$\frac{\rho740-\rho720}{20}$	$\frac{\rho750-\rho720}{30}$
Total slope	$\frac{\rho740-\rho680}{60}$	$\frac{\rho750-\rho700}{50}$
Chlorophyll absorption index	$\frac{\rho680}{\rho850}$	$\frac{\rho680}{\rho750}$

Where ρ is reflectance at the nominated wavelength

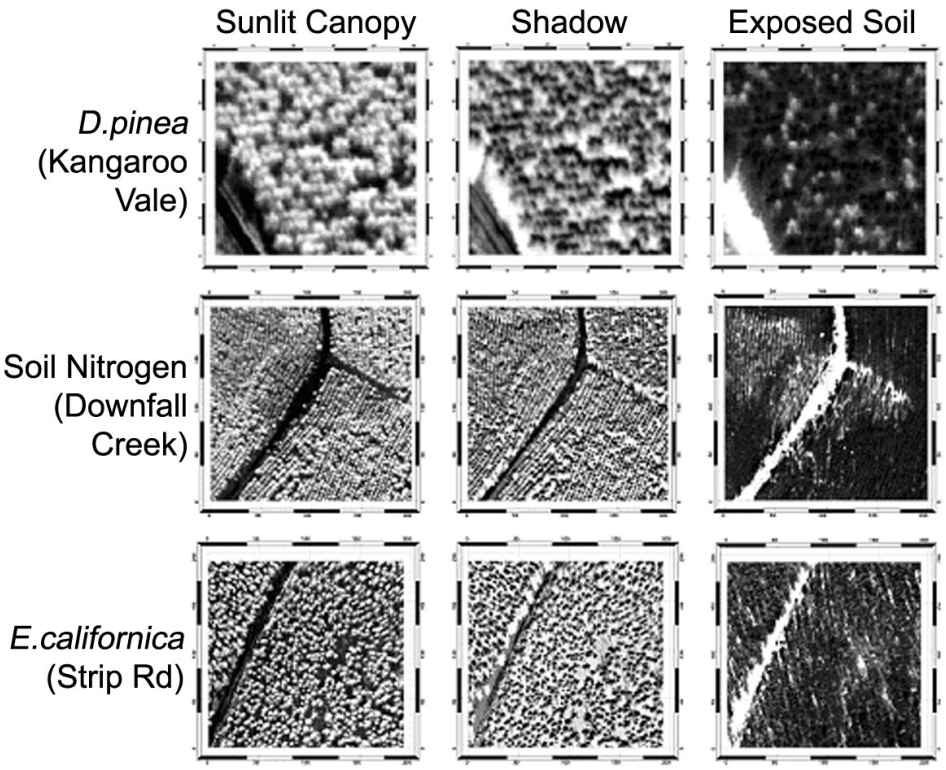

FIG. 2–Sunlit canopy, shadow, and exposed soil fraction images for areas affected by *Diplodia pinea*, low soil nitrogen, and *Essigella californica*.

on a combination of splitting criteria that produced the most consistent groups of crowns in both years.

Ideally, model accuracy should be tested using a secondary data set, collected specifically for model validation purposes and independently of data obtained for the pilot study. The combined nature of the decision tree models meant that it was not possible to assess model accuracy using the recommended v-fold cross validation, the method commonly used for assessing model accuracy based on small data sets in CART (Salford Systems 2003). Instead the accuracy of the models was assessed using an error matrix to compare classifications based on the true condition of the crowns as observed during fieldwork, with the classification indicated by the model. An error matrix shows the number of sampling units (in this case crowns) assigned to a particular category, relative to the actual category as indicated by field data (Congalton 2001). It is possible to obtain a number of metrics of classification accuracy from the error matrix, including overall accuracy (OA) which is the proportion of correct classifications, and the Kappa coefficient which

accounts for chance correlations in its assessment of accuracy (Congalton & Green 1999). Overall accuracy values tend to over-estimate map accuracy (Ma & Redmond 1995) and Kappa analysis tends to under-estimate accuracy (Foody 1992), with the true classification accuracy between the two metrics. Accuracy statistics for individual classes can also be calculated from the error matrices, including error statistics associated with incorrect inclusion (errors of commission or "producer's accuracy") or exclusion (errors of omission or "user's accuracy") in individual classes. This accuracy assessment, while not independent, provides an indication of the accuracy that may be expected using this type of methodology.

Application of the Models

Once the suite of decision tree models, based on tree-scale data, were identified and assessed, the results were applied over larger areas. A two-step crown delineation process was developed within the software package ENVI to extract crown-based information over the entire study area. Firstly, the fractional cover images (derived from the unmixing method) were used to remove pixels with high percentages of soil and shadow. The remaining pixels were then iteratively expanded and smoothed in an image window comparable in size to individual tree crowns. This results in output pixels that are more representative of the mean crown spectral response than individual sub-pixel crown elements. The size of the averaging image window was adjusted according to the average crown size in each image, with a window radius of 8 pixels for the *E.californica* image (average crown diameter 7.8 m) and 3 pixels for the soil deficiency and *D. pinea* images (average crown diameter 3 m).

Finally, once the decision trees were implemented over the entire scene, and estimates of crown health had been derived for each of the damaging factors, the spatial predictions were compared to a range of site, soil, and climatic GIS layers to investigate whether there was any broad-scale relationship between environmental and climatic information and crown condition. To do this a continuous coverage showing the proportion of "unhealthy" to "healthy" crowns within 25-m pixels was created. Grid cells of the raster-transformed *E. californica* crown transparency data were correlated to 32 spatial coverages of climatic, soil, geology, and terrain variables for Kangaroo Vale and Strip Rd in the Carabost State Forest (P.J.Ryan & A.N.Loughhead, CSIRO Forestry & Forest Products, unpubl. data) and the Pearson's correlation coefficients were compared.

RESULTS

A number of decision tree models were developed for each damaging agent. For brevity, one model illustrating a different aspect of the modelling process is presented for each damaging agent.

Presence of Crown Discoloration: *Diplodia pinea*

The best discriminator of crown discoloration caused by *D. pinea* was the upper slope of the red edge, with shallower slopes (<0.006) indicative of significant crown discoloration (proportion of crown with non-green foliage >40) (Fig. 3a). The decision tree produced a simple one-branch model with no other spectral or fraction attributes adding additional discriminating information. A false-colour subset of the *D. pinea*-affected site shows crowns that are severely affected by *D. pinea* in red (Fig. 4a). The same subset is shown in Fig. 4b with pixel values transformed to show the presence of discoloration according to the decision tree model shown in Fig. 3a. The classification error matrix (Table 3) indicates that this model identifies crown discoloration with a true accuracy between 83% (Kappa) and 92% (OA) and with few errors of commission (producer's accuracy 92%) or omission (minimum user's accuracy 87%) in each class.

Crown Volume: Nitrogen Deficient Crowns

The best discriminator of crown volume (m^3) at the low soil-nitrogen site was the sunlit canopy fraction, with fraction values greater than 0.5 (equating to crowns with more than 50% in open sunlight) indicating larger crown volumes (>25 m^3) (Fig. 3b). The effect of low soil nitrogen on crown volume is shown in Fig. 4c, with the smallest crowns (<25 m^3) growing in the most severely nitrogen-depleted areas. This, in turn, increases the visibility of the soil background and understorey compared to areas with higher soil nitrogen levels. The area of most severe soil nitrogen deficit is clearly evident in the decision tree image (Fig. 4d) based on the extent of low-volume crowns. Field checking of the decision tree image showed that the "finger" of higher volume crowns extending from south to north in the western part of the image occurs along a former windrow, where decaying plant material and the ash bed may supplement soil nitrogen levels locally.

TABLE 3–Error matrix showing the classification accuracy of predicting crown discoloration by *Diplodia pinea* (Kappa = 83%, OA = 92%, *N* = 70).

		Observed		User's accuracy (%)
		0–40%	41–100%	
Predicted	0–40%	**57**	3	95
	41–100%	5	**33**	87
Producer's accuracy (%)		92	92	

The error matrix for the crown volume model (Table 4) indicates that it discriminates between high- and low-volume crowns with a true accuracy between 21% (Kappa)

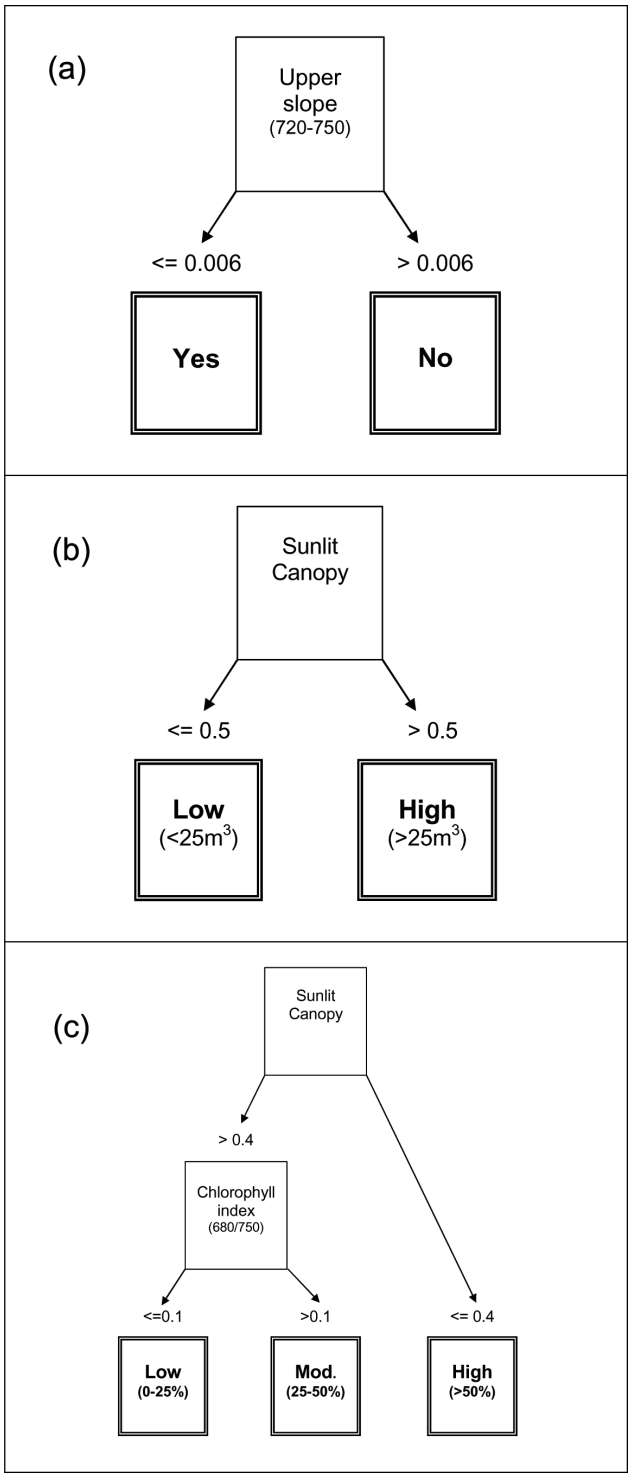

FIG. 3–Decision tree model structures for (a) the presence of discoloration in crowns affected by *Diplodia pinea*, (b) the conical volume of crowns growing in low soil nitrogen, and (c) the mean transparency of crowns affected by *Essigella californica*.

TABLE 4–Error matrix showing the classification accuracy of predicting the conical volume (m^3) of crowns growing in areas of low soil nitrogen (Kappa = 21%, OA = 58%, N = 90).

		Observed		User's
		0–25 m^3	>25 m^3	accuracy (%)
Predicted	0–25 m^3	**40**	1	98
	>25 m^3	37	**12**	24
Producer's accuracy (%)		52	92	

and 58% (OA) with a tendency to over-estimate crown volume. Large volume crowns were correctly classified in 92% of cases (producer's accuracy), but only 24% of crowns classified as having a large volume were actually large crowns according to the field data (user's accuracy).

Mean Crown Transparency: *Essigella californica*

The model for mean crown transparency in crowns affected by *E. californica* splits crowns into three transparency classes (high > 50%; moderate 25–50%; low 0–25%) (Fig. 3c and 4c). The major discriminator of mean crown transparency is sunlit canopy, with small fractional values indicating highly transparent crowns. The minor discriminator, which splits crowns into groups of lower transparency levels, is the chlorophyll index, with higher index values corresponding to more transparent crowns. The results show highly transparent crowns are relatively evenly distributed throughout the subset image; this is typical as *E. californica* tends to attack crowns over a large area under favourable conditions (Neumann & Marks 1990; Nambiar & Booth 1991; May & Carlyle 2003). The proportion of high transparency crowns throughout the Strip Rd image is shown in Fig. 5.

The classification error matrix for this model (Table 5) indicates a true classification accuracy between 28% (Kappa) and 68% (OA) tending towards an over-estimation

TABLE 5–Error matrix showing the classification accuracy of predicting the mean transparency (%) of crowns affected by *Essigella californica* (Kappa = 28%, OA = 68%, N = 94).

		Observed			User's
		0–25%	25–50%	>50%	accuracy (%)
Predicted	0–25%	**6**	10	0	38
	25–50%	10	**62**	8	78
	>50%	0	8	**8**	50
Producer's accuracy (%)		38	78	50	

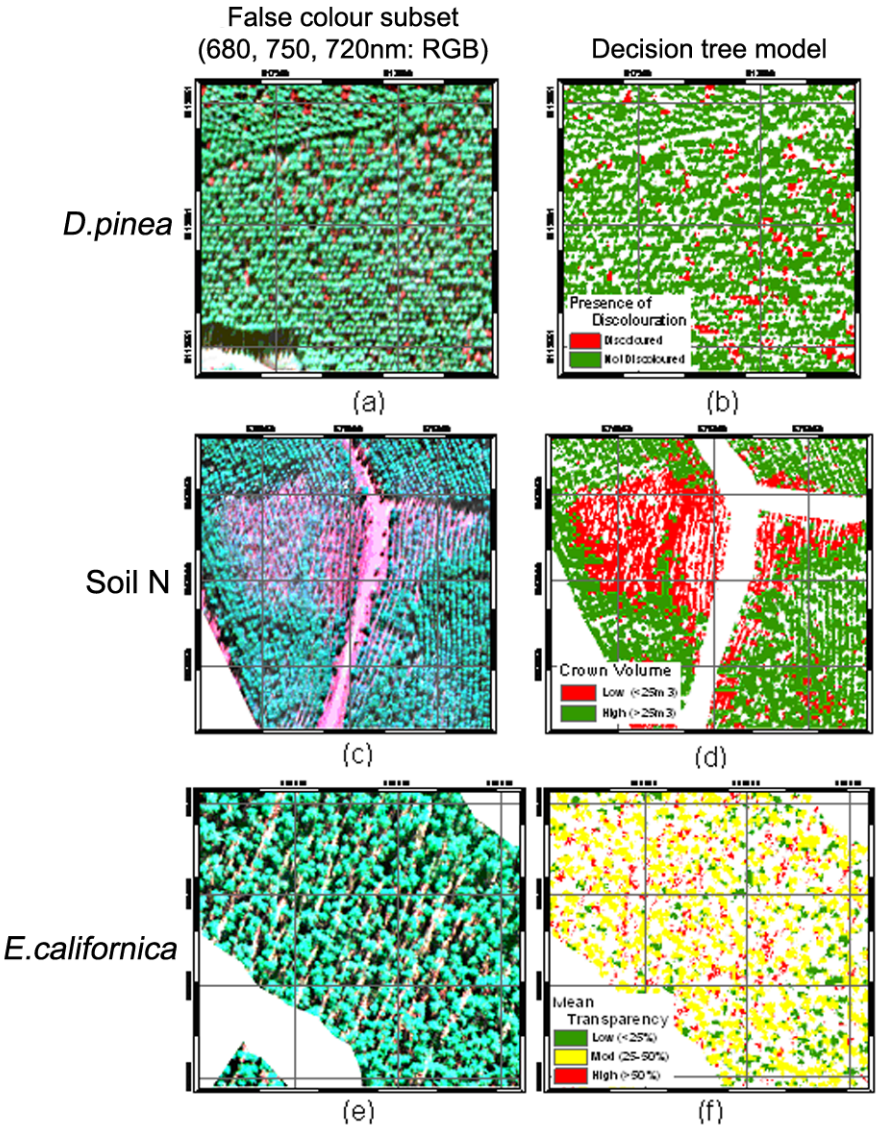

FIG. 4–False colour and decision tree model images showing the *Diplodia pinea* site (a) and the presence of discolouration model (b), the low soil nitrogen site (c) and the crown volume model (d), and the *Essigella californica* site (e) and the mean crown transparency model (f).

of the transparency of the least affected crowns. A subset of the *E. californica* scene in false colour is shown in Fig. 4e and the model results are shown in Fig. 4f.

A total of 32 spatial variables were derived for correlation with the raster-transformed *E. californica* crown transparency coverage, including a series of attributes derived

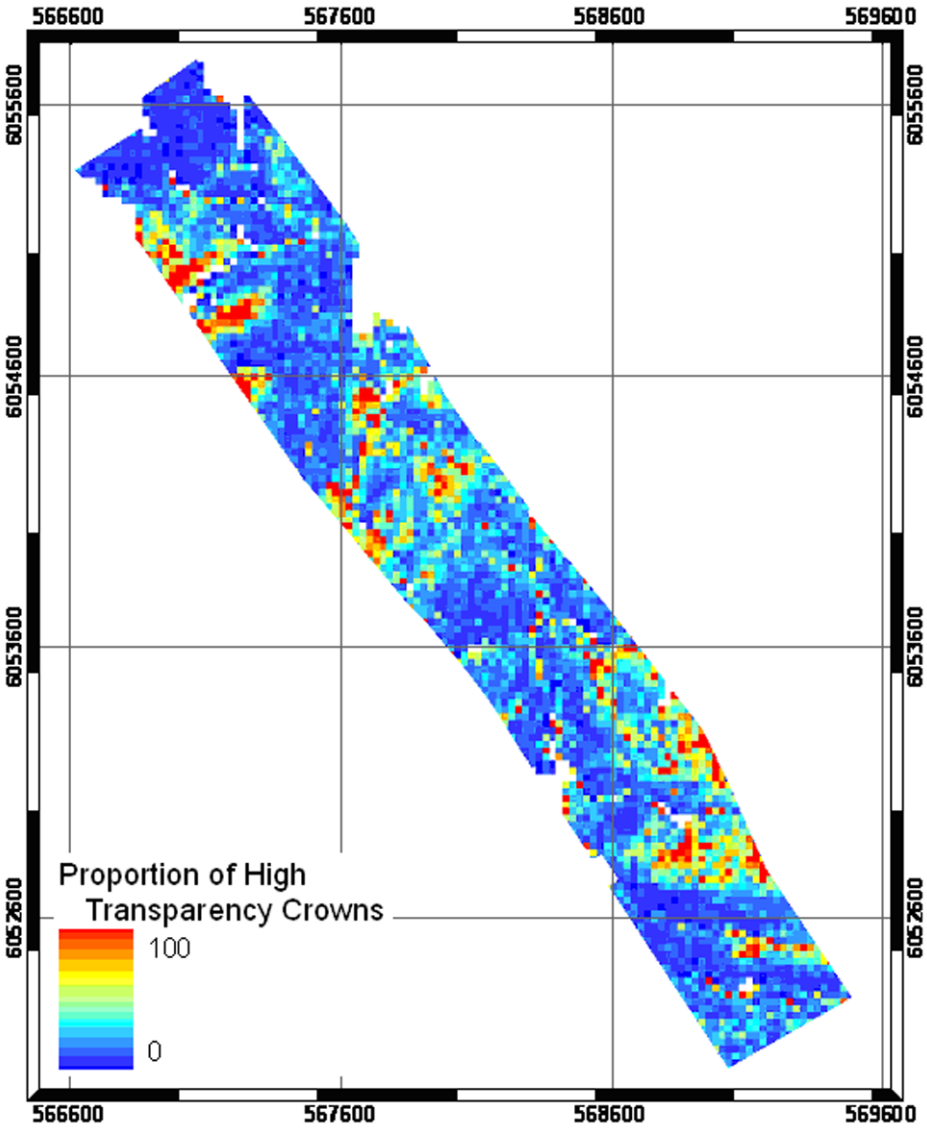

FIG. 5–The proportion of crowns infested with *Essigella californica* in the high transparency class to crowns in the low and moderate transparency classes in the Strip Rd study area in 2002.

from digital elevation models — geophysical remote sensing of gamma radiometric data and the profile available water-holding capacity, a measure of potential soil water stress (McKenzie & Ryan 1999; Ryan *et al.* 2000). Significant correlates were elevation ($r = 0.17$, $p<0.0001$), radiometric potassium ($r = 0.17$, $p<0.0001$), and the natural logarithm of the dispersive area ($r = 0.16$, $p<0.0001$). The most

significant correlation between the relative proportion of high transparency crowns and site/soil attributes was with net radiation using an exponential transformation ($r = 0.32$, $p<0.0001$; Fig. 6). Areas with northerly or north-west aspects (and of higher elevation) are exposed to relatively higher net radiation levels and these locations also have a greater proportion of highly transparent crowns infested with *E. californica*.

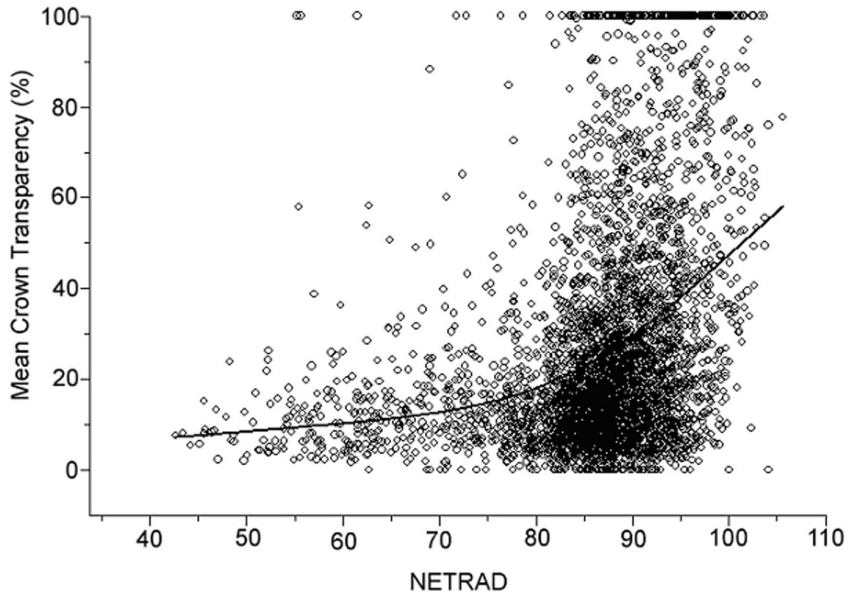

FIG. 6–Correlation between Fig. 5, and annual net solar radiation ($r = 0.32$).

DISCUSSION

At present, most plantation health assessment data are collected by subjective methods such as aerial and ground-based visual surveys (e.g., White *et al*. 2005). To meet the increasing demands of profitability, quality assurance, and environmental stewardship, however, plantation managers will require access to more precise data describing the status of their estates (Stone & Coops 2004). This pilot study demonstrated that narrow-band high-resolution multi-spectral imagery can detect a range of tree crown symptoms associated with *P. radiata* in southern New South Wales, including crown discoloration, defoliation, and reduced crown size. Spatial quantification of these damage symptoms is required to accurately determine the impact on stand productivity from damaging agents such as pests and diseases, and to assess their financial implications.

The current cost of acquiring and processing high-resolution digital multi-spectral imagery is approximately $2.00 to $5.00/ha depending on detail and analytical

requirements (Andrew Malcolm, SpecTerra Services Pty Ltd, Leederville, Western Australia, pers. comm.). This is more expensive than that quoted for GPS aerial-sketch mapping provided by the forest health surveillance unit of Forests New South Wales (Angus Carnegie, Forests NSW, Sydney, pers. comm.). However, the subjective coarse nature of the information collected by forest health surveillance units is not easily incorporated into existing (or developing) forest management systems, and associated accuracies are rarely reported. In addition, analyses of the kind demonstrated in this article are likely to become considerably cheaper in future due to the increasing availability of high spatial resolution multi-spectral imagery from satellite sensors.

Decision tree analysis was selected for this study because it has several advantages over traditional regression, including the fact that it is not based on linear and additive relationships between factors, and variables do not need to fulfill distributional assumptions. Explanatory variables can be used in their original format including categorical data (Rosso & Hansen 2004), which significantly improves the intuitive interpretation of crown health models. Decision tree models are best suited for use with large data sets, however, which can be separated into model construction and model validation components. The small sample sizes in this analysis meant that decision tree models were based on the entire sample of crowns. While the error matrices, therefore, probably over-estimate the accuracy of the models (Congalton & Green 1999), a more realistic interpretation of classification accuracy has been achieved through the use of both overall accuracy which tends to over-estimate classification accuracy, and Kappa coefficients which tend to under-estimate accuracy. We recommend that both the overall accuracy and Kappa statistics should be used to assess classification accuracy in future analyses of this kind.

As with any programme which utilises airborne remote sensing imagery, the timing of image acquisition is critical. As discussed, the importance of obtaining imagery just prior to new shoot growth was judged the overriding priority in flight planning. As a result the sun angle, and therefore the proportion of sunlit crown and shadow, will be different from imagery obtained in summer. The decision to fly in September may, therefore, have an adverse effect on the prediction of the fraction images from imagery obtained in summer. To avoid this problem this study design utilised only imagery collected on approximately the same date each year. If these models were to be applied to imagery acquired at other times of the year they may need to be recalibrated to ensure accurate results.

This application of remotely sensed imagery illustrates advantages of spatially explicit high-resolution digital remote sensing for canopy health assessment in *P. radiata* — in particular, its potential for quantitative analysis at a range of scales and with respect to other digital spatial coverages within a GIS framework. These

characteristics provide the immediate potential for integrated visualisation and modelling of various spatial layers across a range of operational and environmental scales. The model of mean crown transparency in *E.californica*-damaged trees was easily applied over the entire image for correlation analysis with other data in a GIS, for example. This information can then form the basis of site hazard ratings for a range of commercially important pests and diseases, or assist in targeting plantation management practices by identifying environmental attributes associated with the distribution of damaging agents. In addition to management applications, tree-based decision tools using remotely sensed canopy condition, geo-referenced climate, and topographic and soil information can provide quantitative insight into the behaviour of damaging agents. The association described in this study between the mean crown transparency of *E. californica*-damaged trees and net radiation levels (Fig. 5) is similar to that reported by Appleton *et al. (*2003) in New Zealand which found higher aphid populations on trees growing on north-facing sunny aspects than on other aspects.

While the restricted nature of this study limits extrapolation across space and time, the results nevertheless indicate that the use of high spatial multi-spectral imagery to assess *P. radiata* canopy health warrants further investigation. Improvements in model accuracy can be achieved through a range of analytical techniques such as stratification of the imagery with existing GIS plantation inventory information in order to constrain variability due to stand management practices (e.g., Hall *et al*. 2003). As with current forest health assessment programmes, the accompanying ground-sampling will always be expensive and spatially incomplete. For example, the incorporation of remotely acquired imagery with optical radiative transfer models (e.g., Zarco-Tejada *et al*. 2004; Rautiainen 2005) and process-based models (e.g., Coops *et al*. 2001) may off-set some of this reliance on ground sampling in the future.

ACKNOWLEDGMENTS

This work is one of the outcomes from a collaborative research project between CSIRO Forestry and Forest Products and State Forests of New South Wales, supported and partially funded by the Forest and Wood Products Research and Development Corporation (PN02.1906). The authors acknowledge the tremendous assistance of Grahame Price, Angus Carnegie, and Ian Hides (SFNSW) and Michael Stanford, Ken Old, Mark Dudinski, Darius Culvenor, and Nick Goodwin (Ensis) with field data and imagery collection. The authors also acknowledge the assistance of Barrie May (Ensis), Ross Dickson (SFNSW), and Andrew Haywood (formerly of SFNSW) who commented on a draft of this paper.

REFERENCES

APPLETON, C.; GRESHAM, B.A.; ZYDENBOS, S.M. 2003: Monitoring *Essigella californica* populations in Bay of Plenty forests. *New Zealand Plant Protection 56*: 45–50.

ASRAR, G. 1989: "Theory and Applications of Optical Remote Sensing". John Wiley and Sons, New York.

CARLYLE, C.; NAMBIAR, E.K.S. 2001: Relationships between net nitrogen mineralization, properties of the forest floor and mineral soil, and wood production in *Pinus radiata* plantations. *Canadian Journal of Forest Research 31*: 889–898.

CARVER, M.; KENT, D.S. 2000: *Essigella californica* (Essig) and *Eulachnus thunbergii* Wilson (Hemiptera: Aphididae: Lachninae) on *Pinus* in south-eastern Australia. *Australian Journal of Entomology 39*: 62–69.

CONGALTON, R.G. 2001: Accuracy assessment and validation of remotely sensed and other spatial information. *International Journal of Wildland Fire 10*: 321–328.

CONGALTON, R.G.; GREEN, K. 1999: "Assessing the Accuracy of Remotely Sensed Data: Principles and Practices". Lewis Publishers, London.

COOPS, N.C.C.; STONE, C. 2005: A comparison of field-based and modelled reflectance spectra from damaged *Pinus radiata* foliage. *Australian Journal of Botany 53*: 1–13.

COOPS, N.C.C.; WARING, R.H.; LANDSBERG, J.J. 2001: Estimation of potential forest productivity across the Oregon transect using satellite data and monthly weather records. *International Journal of Remote Sensing 22*: 3797–3812.

COOPS, N.C.C.; STONE, C.; CULVENOR, D.S.; CHISHOLM, L. 2004: Assessment of crown condition in eucalypt vegetation by remotely sensed optical indices. *Journal Environment Quality 33*: 956–964.

COOPS, N.C.C.; STANFORD, M.; OLD, K.; DUDZINSKI, M.; CULVENOR, D.S.; STONE, C. 2003: Assessment of Dothistroma needle blight of *Pinus radiata* using airborne hyperspectral imagery. *Phytopathology 93*: 1524–1532.

CURRAN, P.J.; DUNGAN, J.L.; GHOLZ, H.L. 1990: Exploring the relationship between reflectance red edge and chlorophyll content in slash pine. *Tree Physiology 7*: 33–48.

FITZGERALD, G.J.; MAAS, S.J.; DETAR, W.R. 2002: Detecting spider mite damage in cotton through spectral mixture analysis of AVIRIS imagery. *In* "Proceedings of the 11th Airborne Visible/Infrared Imaging Spectrometer (AVIRIS) Workshop". Jet Propulsion Laboratory, Pasadena, CA.

FOODY, G.M. 1992: On the compensation for chance agreement in image classification accuracy assessment. *Photogrammetric Engineering and Remote Sensing 58*: 1459–1460.

FRANKLIN, S.E. 2000: "Remote Sensing for Sustainable Forest Management". Lewis Publishers, Boca Raton

FRIEDL, M.A.; BRODLEY, C.E. 1997: Decision tree classification of land cover from remotely sensed data. *Remote Sensing Environment 61*: 399–409.

FURBY, S.L.; CAMPBELL, N.A. 2001: Calibrating images from different dates to 'like value' digital counts. *Remote Sensing of Environment 77*: 1–11.

GAUSMAN, H.W. 1985: Plant leaf optical properties in visible and near-infrared light. *Graduate Studies, Texas Technical University No. 29*. 78 pp.

GOODWIN, N.; COOPS, N.C.C.; STONE, C. 2005: Assessing plantation canopy condition from airborne imagery using spectral mixture analysis and fractional abundances. *International Journal of Applied Earth Observation and Geoinformation 7*: 11–28.

HALL, R.J.; FERNANDES, R.A.; HOGG, E.H.; BRANDT, J.P.; BUTSON, C.; CASE, B.S.; LEBLANC, S.G. 2003: Relating aspen defoliation to changes in leaf area derived from field and satellite remote sensing data. *Canadian Journal Remote Sensing 29*: 299–313.

HANSEN, M.; DUBAYAH, R.; DEFRIES, R.S. 1996: Classification trees: an alternative to traditional land cover classifiers. *International Journal Remote Sensing 17*: 1075–1081.

KNIPLING, E.B. 1970: Physical and physiological basis for the reflectance of visible and near infrared radiation from vegetation. *Remote Sensing of the Environment 1*: 155–159.

LAWRENCE, R.; WRIGHT, A. 2001: Rule-based classification systems using Classification and Regression Trees (CART) Analysis. *Photogrammetry Engineering and Remote Sensing 67*: 1137–1142.

LECKIE, D.G.; CLONEY, E.; JOYCE, S.P. 2005: Automated detection and mapping of crown discolouration caused by jack pine budworm with 2.5 m resolution multispectral imagery. *International Journal of Applied Earth Observation and Geoinformation 7*: 61–77.

LECKIE, D.G.; YUAN, X.; OSTAFF, D.P.; PIENE, H.; MACLEAN, D.A. 1992: Analysis of high resolution multispectral MEIS imagery for spruce budworm damage assessment on a single tree basis. *Remote Sensing of Environment 40*: 125–136.

LEES, B.G. 1994: Decision trees, artificial neural networks and genetic algorithms for classification of remotely sensed and auxiliary data. Pp. 51–60 *in* "Proceedings of the 7th Australasian Remote Sensing Conference", Melbourne.

LÉVESQUE, J.; KING, D.J. 2003: Spatial analysis of radiometric fractions from high-resolution multispectral imagery for modelling forest structure and health. *Remote Sensing of Environment 84*: 589–602.

MA, Z.; REDMOND, R. 1995: Tau coefficients for accuracy assessment of classification of remote sensing data. *Photogrammetric Engineering and Remote Sensing 61*: 435–439.

MARTIN, M.E.; ABER, J.A. 1997: High spectral resolution remote sensing of forest canopy lignin, nitrogen, and ecosystem processes. *Ecological Applications 7*: 431–443.

MAY, B.M.; CARLYLE, J.C. 2003: Effect of defoliation associated with *Essigella californica* on growth of mid-rotation *Pinus radiata*. *Forest Ecology and Management 183*: 297–312.

McCONNELL, T.J.; JOHNSON, E.W.; BURNS, B. 2000: A guide to conducting aerial sketchmapping surveys. *USDA Forest Service, Forest Health Technology Enterprise Team, Report number FHTET 00-001.*

McKENZIE, N.J.; RYAN, P.J. 1999: Spatial prediction of soil properties using environmental correlation. *Geoderma 89*: 67–94.

NAMBIAR, E.K.S.; BOOTH, T.H. 1991: Environmental constraints on the productivity of eucalypt and pine: Opportunities for site management and breeding. Pp. 215–231 *in* Proceedings of the "Productivity in Perspective": 3rd Australian Forest Soils and Nutrition Conference, Melbourne, Forestry Commission of N.S.W., Sydney.

NEUMANN, F.G.; MARKS, G.C. 1990: Status and management of insect pests and diseases in Victorian softwood plantations. *Australian Forestry 53*: 131–144.

PEDDLE, D.R.; HALL, F.; LEDREW, E.F. 1999: Spectral mixture analysis and geometric optical reflectance modeling of boreal forest biophysical structure. *Remote Sensing of Environment 67*: 288–297.

PONTIUS, J.; HALLETT, R.; MARTIN, M. 2005: Using AVIRIS to assess hemlock abundance and early decline in the Catskills, New York. *Remote Sensing of Environment 97*: 163–173.

PU, R.; YU, Q.; GONG, P.; BIGING, G.S. 2005: EO-1 Hyperion, ALI and Landsat 7 ETM+ data comparison for estimating forest crown closure and leaf area index. *International Journal of Remote Sensing 26*: 457–474.

RAUTIANEN, M.; STENBERG, P.; NILSON, T.; KUUSK, A. 2004: The effect of crown shape on the reflectance of coniferous stands. *Remote Sensing of Environment* 89: 41–52.

ROBERTS, D.A.; SMITH, M.O.; ADAMS, J.B. 1993: Green vegetation, nonphotosynthetic vegetation, and soils in AVIRIS data. *Remote Sensing Environment 44*: 255–269.

ROSSO, P.H.; HANSEN, E.M. 2004: Predicting swiss needle cast distribution and severity in young Douglas-fir plantations in coastal Oregon. *Phytopathology 93*: 790–798.

RSI (RESEARCH SYSTEMS INSTITUTE) 2003: "Environment for Visualizing Images (ENVI) System Manual". RSI Inc., Pearl East Circle, Boulder, CO 80301, USA.

RYAN, P.J.; McKENZIE, N.J.; O'CONNELL, D.O.; LOUGHHEAD, A.N.; LEPPART, P.M.; JACQUIER, D.; ASHTON, L. 2000: Integrating forest soil information across scales: spatial prediction of soil properties under Australian forest. *Forest Ecology and Management 138*: 139–157.

SALFORD SYSTEMS 2003: "CART 5, Version 5. Salford Systems". San Diego, California.

SCHLERF, M.; ATZBERGER, C.; HILL, J. 2005: Remote sensing of forest biophysical variables using HyMap imaging spectrometer data. *Remote Sensing of Environment 95*: 177–194.

SONG, C.; WOODCOCK, C.E.; SETO, K.C.; LENNEY, M.P.; MACOMBER, S.A. 2001: Classification and change detection using Landsat TM data: when and how to correction atmospheric effects. *Remote Sensing of Environment 75*: 230–244.

SPECTERRA SERVICES 2004: "Digital Multi-Spectral Imagery (DMSI): Technical specifications". Specterra Services, Leederville, Western Australia.

STANOSZ, G.R. 1997: Sphaeropsis shoot blight and canker. Pp. 42–43 *in* Hansen, E.M.; Lewis, K.J. (Ed.) "Compendium of Conifer Diseases". American Phytopathological Society, St. Paul, M.N., U.S.A.

STONE, C.; COOPS, N.C.C. 2004: Assessment and monitoring of damage from insects in Australian eucalypt forests and commercial plantations. *Australian Journal of Entomology 43*: 282–292.

THENKABAIL, P.S.; SMITH, R.B.; DE PAUW, E. 2000: Hyperspectral vegetation indices and their relationship with agricultural crop characteristics. *Remote Sensing of Environment 71*: 158–182.

TOMPKINS, S.; MUSTARD, J.F.; PIETERS, C.M.; FORSYTH, D.W. 1997: Optimization of endmembers for spectral mixture analysis. *Remote Sensing Environment 59*: 472–489.

USDA FOREST SERVICE 2002: "Forest Inventory and Analysis: National Core Field Guide, 1: Field Data Collection Procedures for Phase 2 Plots, Version 1.6". US Department of Agriculture Forest Service, Forest Inventory and Analysis, Washington.

YANG, X.; LO, C.P. 2000: Relative radiometric normalization performance for change detection from multi-date satellite images. *Photogrammetrical Engineering Remote Sensing 66*: 967–981.

WHARTON, T.N.; KRITICOS, D.J. 2004: The fundamental and realised niche of the Monterey pine aphid *Essigella californica* (Essig) (Hemiptera: Aphidae): implications for managing softwood plantations in Australia. *Diversity and Distributions 10*: 253–262.

WHITE, J.D.; RUNNING, S.W.; NEMANI, R.; KEANE, R.E.; RYAN, C.R. 1997: Measurement and remote sensing of LAI in Rocky Mountain montane ecosystems. *Canadian Journal Forest Research 27*: 1714–1727.

WHITE, J.C.; WULDER, M.A.; BROOKS, D.; REICH, R.; WHEATE, R.D. 2005: Detection of red attack stage mountain pine beetle infestation with high spatial resolution satellite imagery. *Remote Sensing of Environment 96*: 340–351.

WILL, G. 1985: Nutrient deficiencies and fertiliser use in New Zealand exotic forests. *New Zealand Forest Service, Forest Research Institute, FRI Bulletin No. 97.*

ZARCO-TEJADA, P.J.; PUSHNIK, J.C.; DOBROWSKI, S.; USTIN, S.L.. 2003: Steady-state chlorophyll *a* fluorescence detection from canopy derivative reflectance and *double-peak* red-edge effects. *Remote Sensing of Environment 84*: 283–294.

ZARCO-TEJADA, P.J.; MILLER, J.R.; MORALES, A.; BERJÓN, A.: AGÜERA, J. 2004: Hyperspectral indices and model simulation for chlorophyll estimation in open-canopy tree crops. *Remote Sensing of Environment 90*: 463–476.